J. Fluid Mech. (1974), *vol.* 65, *part* 1, *pp.* 113–125
Printed in Great Britain

The effects of surface roughness and tunnel blockage on the flow past spheres

By ELMAR ACHENBACH

Institut für Reaktorbauelemente der Kernforschungsanlage Jülich GmbH, Jülich, Germany

(Received 7 December 1973)

The effect of surface roughness on the flow past spheres has been investigated over the Reynolds number range $5 \times 10^4 < Re < 6 \times 10^6$. The drag coefficient has been determined as a function of the Reynolds number for five surface roughnesses. With increasing roughness parameter the critical Reynolds number decreases. At the same time the transcritical drag coefficient rises, having a maximum value of 0·4.

The vortex shedding frequency has been measured under subcritical flow conditions. It was found that the Strouhal number for each of the various roughness conditions was equal to its value for a smooth sphere. Beyond the critical Reynolds number no prevailing shedding frequency could be detected by the measurement techniques employed.

The drag coefficient of a sphere under the blockage conditions $0{\cdot}5 < d_s/d_t < 0{\cdot}92$ has been determined over the Reynolds number range $3 \times 10^4 < Re < 2 \times 10^6$. Increasing blockage causes an increase in both the drag coefficient and the critical Reynolds number. The characteristic quantities were referred to the flow conditions in the smallest cross-section between sphere and tube. In addition the effect of the turbulence level on the flow past a sphere under various blockage conditions was studied.

1. Introduction

In a previous paper by Achenbach (1972) the effect of the Reynolds number on the flow past smooth spheres was studied up to very high Reynolds numbers ($Re = 6 \times 10^6$). It was expected that the flow might be influenced by the surface conditions of the sphere and, therefore, great importance was attached to producing very smooth surfaces. This paper describes the second part of those experiments, in which the effects of surface roughness were examined. This topic is not dealt with in the available literature.

The effect of tunnel blockage has been studied in connexion with the problem of the pneumatic transport of a single sphere in a tube. Only high blockage ratios $0{\cdot}5 < d_s/d_t < 0{\cdot}92$, where d_s is the diameter of the sphere and d_t the diameter of the tube, were considered.

It is well known that the drag coefficient of a sphere in an infinite flow drops considerably when the critical flow range is reached. The problem was to determine whether, for high blockage ratios, such a critical Reynolds number exists

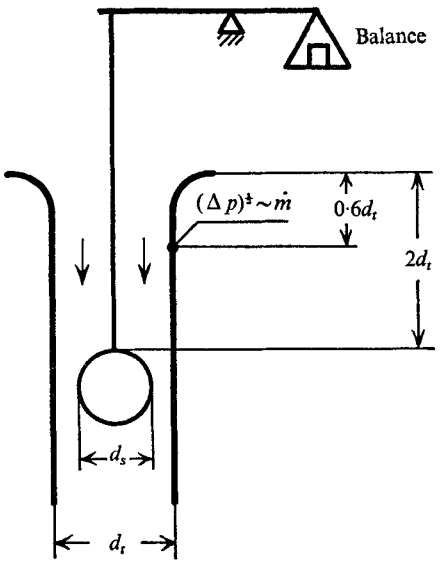

FIGURE 1. Experimental arrangement for blockage tests; $d_t = 0{\cdot}191$ m.

and, if it does, how its value depends on the blockage ratio. From the practical point of view it must be established that in any flow state the drag forces are strong enough to cause safe transport of the sphere.

The experimental results indicated the existence of a critical Reynolds number range even for the highest blockage ratios. The tests were effected by measuring the local static pressure and skin friction under the blockage condition $d_s/d_t = 0{\cdot}916$.

2. Experimental apparatus and measurement techniques

For the determination of the drag coefficient as a function of the Reynolds number and roughness parameter k/d_s, where k is the height of the roughness elements, the same experimental techniques were applied as those described in the paper on the flow past smooth spheres (Achenbach 1972). The high Reynolds numbers were realized using a high-pressure wind tunnel. The drag forces were measured by means of a balance incorporating a strain-gauge bridge. This balance was mounted within the hollow test sphere. The sphere had a diameter of about 0·2 m and was supported from the rear by a sting which was 0·75 m long.

In four of the tests, the rough surface was obtained by pasting glass spheres of diameter k onto the surface; the sizes chosen were $k = 2{\cdot}5 \times 10^{-3}$, 1×10^{-3}, $0{\cdot}5 \times 10^{-3}$ and $0{\cdot}3 \times 10^{-3}$ m. In a further test, a smaller roughness height was produced by abrading the surface with coarse emery paper: an irregular pattern of grooves about 5×10^{-5} m deep was formed. The roughness height k is divided by the sphere diameter d_s to obtain the roughness parameter k/d_s. With the roughness heights mentioned above the following values of the roughness parameter result: $k/d_s = 1250 \times 10^{-5}$, 500×10^{-5}, 250×10^{-5}, 150×10^{-5} and 25×10^{-5}.

A sketch of the apparatus in which the effect of tunnel blockage was investi-

gated is illustrated in figure 1. The sphere was suspended from a balance by means of a wire. Thus the total drag force F could be measured directly. The mass flow $\dot{m}$ was calculated from the pressure drop at the entrance of the tube. The corresponding inlet coefficient was determined to be $\alpha = 0{\cdot}97$. The local static pressure and the wall shear stresses were measured using a test sphere from previous investigations which was equipped with a calibrated skin-friction probe (Achenbach 1972). The probes were inserted in a rotatable ring-shaped element of the sphere and could be placed at any circumferential position. The vortex shedding frequency was indicated by hot wires which were mounted flush with the surface of the sphere. This technique had been employed in previous experiments (Achenbach 1974). It was found then that the optimum angular position for installing the probe is $\phi = 75°$, ϕ being measured from the front stagnation point. The hot-wire signals were relayed to a frequency analyser.

During the investigation of the blockage effect, the turbulence level of the incident flow was varied by mounting screens of different mesh size in the inlet section. The turbulence level T, which is defined as

$$T = (\overline{u'^2})^{\frac{1}{2}}/U,$$

where U is the mean velocity in the entrance, was measured by means of a hot wire.

3. Results

3.1. *The effect of surface roughness on the drag on spheres*

Roughness elements distributed on the surface of a body in a fluid stream cause transition from laminar to turbulent flow if the disturbances generated by them are amplified. For bluff bodies without salient edges to fix the separation points, the premature onset of turbulence in the boundary layer causes a shift of the separation point and hence a change in the drag forces. This effect has been demonstrated for a circular cylinder in a cross-flow. A similar result was expected for the sphere.

In figure 2 the drag coefficient c_d of the sphere is plotted as a function of the Reynolds number for various roughness parameters k/d_s. With increasing roughness parameter the critical Reynolds number Re_c, defined as the value where c_d is a minimum, decreases (see also figure 3). For subcritical conditions the curves corresponding to the particular roughnesses collapse. At a certain value of the Reynolds number which is dependent on the roughness parameter, the drag coefficient decreases rapidly. This is the critical flow range where small variations in the Reynolds number cause considerable changes in the drag coefficient. Beyond the critical Reynolds number the drag coefficient increases again. This range is defined to be the supercritical flow range. It is succeeded by the transcritical regime, where the drag coefficient is nearly independent of the Reynolds number. The boundary between the supercritical and transcritical flow regimes is floating. This has already been mentioned in the paper on the flow past smooth spheres. The transcritical flow is characterized by a more or less constant value of the drag coefficient for each roughness. It appears that there exists a maximum

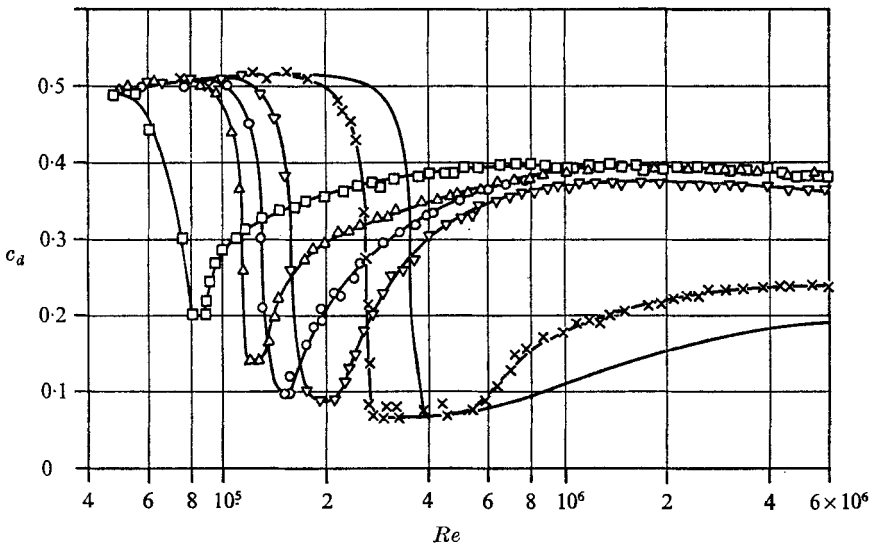

FIGURE 2. Drag coefficient c_d *vs.* Reynolds number for a sphere. Parameter: surface roughness. ——, smooth (Achenbach 1972); ×, $k/d_s = 25\times10^{-5}$; ▽, $k/d_s = 150\times10^{-5}$; ○, $k/d_s = 250\times10^{-5}$; △, $k/d_s = 500\times10^{-5}$; □, $k/d_s = 1250\times10^{-5}$.

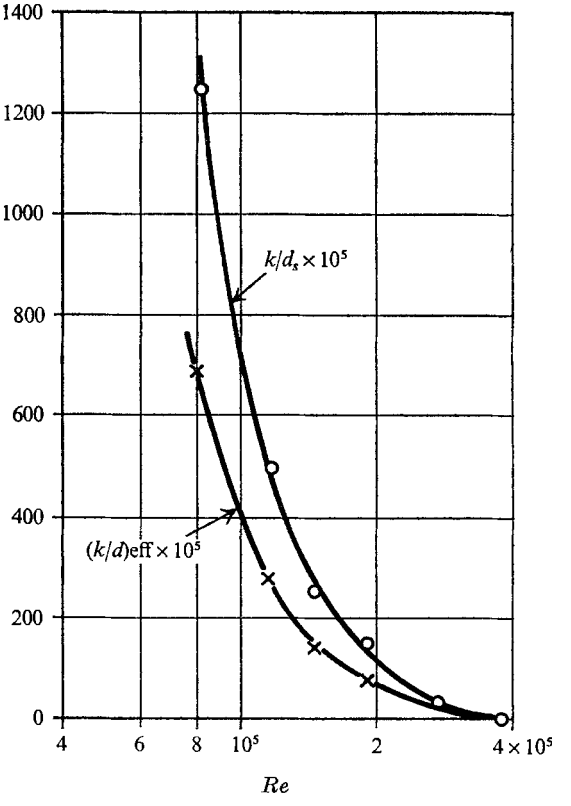

FIGURE 3. Roughness parameter *vs.* critical Reynolds number. ×, $(k/d)_{\text{eff}}$, see §4.

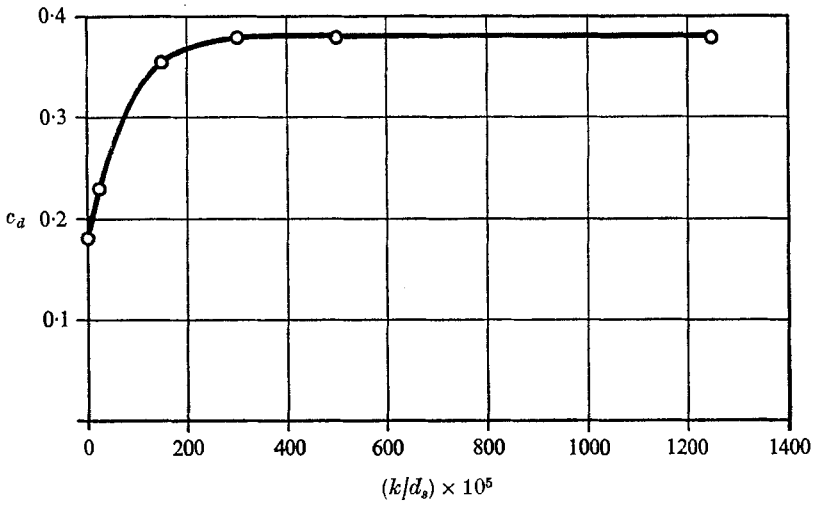

FIGURE 4. Transcritical drag coefficient *vs.* roughness parameter for a sphere. $Re = 5 \times 10^6$.

value of the drag coefficient which is not exceeded though the roughness parameter increases. In particular this evidence is illustrated in figure 4, which shows the transcritical drag coefficient as a function of the roughness parameter for $Re = 5 \times 10^6$. A similar trend is obvious on considering the results for a rough circular cylinder in a cross-flow (Achenbach 1971). Here the transcritical drag coefficients of the cylinders covered with the two highest roughnesses tested come close together. Recent unpublished results on this point confirm that observation.

Comparison of the flow resistance curves for the rough sphere and a rough circular cylinder in a cross-flow indicates a significant similarity. It therefore appears justifiable to draw similar conclusions concerning the behaviour of the boundary layer on the basis of the drag curves. For subcritical flow conditions the boundary layer separates laminarly. In the critical flow regime the separation point of the boundary layer begins to shift downstream, but laminar separation still occurs. With a further increase in the Reynolds number the free shear layer becomes turbulent and reattaches to the wall. The boundary layer receives energy from outside through turbulent fluctuations. Thus it is able to develop further downstream in spite of a positive pressure gradient. Finally it separates turbulently. The resulting reduction in the width of the wake causes an increase in the static pressure at the rear of the sphere, which leads to the low values of the drag coefficient. In the supercritical flow range the transition from laminar to turbulent flow occurs immediately. The point of transition shifts to the front stagnation point with increasing Reynolds number. At the same time the point of boundary-layer separation moves upstream and causes higher drag coefficients. Under transcritical flow conditions nearly the whole boundary layer is turbulent.

During the tests under atmospheric conditions it was possible to determine the boundary-layer separation by means of the wool-tuft technique. Figure 5 illustrates the dependency of the separation point ϕ_s on the Reynolds number for roughness parameters $k/d_s = 250 \times 10^{-5}$ and 1250×10^{-5}. The values referring to

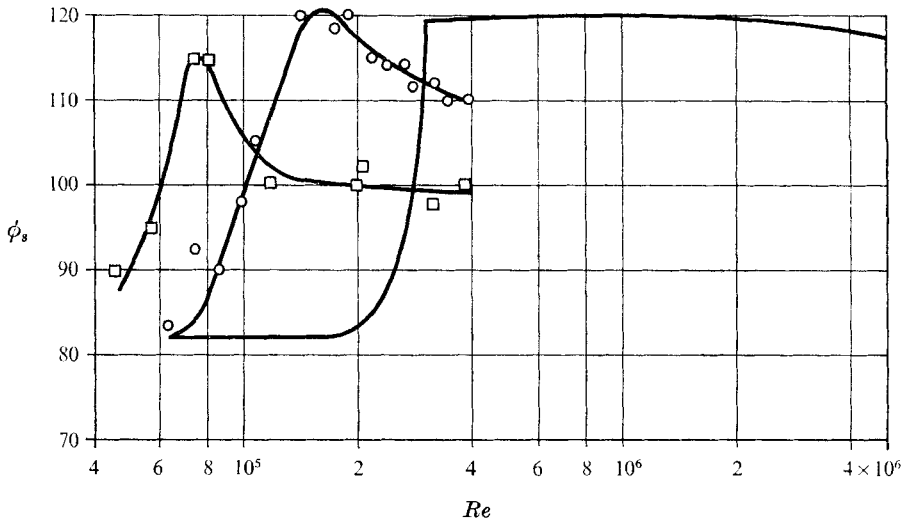

FIGURE 5. Angle ϕ_s of boundary-layer separation *vs.* Reynolds number for a sphere. ——, smooth (Achenbach 1972); ○, $k/d_s = 250\times10^{-5}$; □, $k/d_s = 1250\times10^{-5}$.

the smooth sphere are taken from Achenbach (1972). The accuracy of the method is not very good. However, the characteristic shift of the separation point at critical and supercritical flow conditions described above is evident. The curves have nearly the same shapes as those showing the c_d *vs.* *Re* relationship but inverted.

3.2. *Vortex shedding from rough spheres*

Initially the tests on vortex shedding from rough spheres were intended to study the vortex shedding mechanism in the critical flow range, employing velocities as low as possible. The aim of this was to eliminate the effects of vibration of the sphere which was produced by the powerful fluctuating aerodynamic forces. However, it was found that immediately before the critical Reynolds number was reached the periodic hot-wire signal vanished; this was also observed for the smooth sphere as mentioned by Achenbach (1974). In particular this effect occurred at the Reynolds number where the drag coefficient starts dropping. This fact becomes evident from figure 6 taken together with figure 2. In addition figure 6 indicates that for subcritical flow conditions the Strouhal number based on the vortex shedding frequency f, sphere diameter d_s and free-stream velocity U_∞ is almost identical for rough and smooth spheres.

3.3. *Effect of tunnel blockage*

If the cross-section of the flow is partially blocked by the sphere, the equatorial velocity increases with increasing blockage. The static pressure at the rear of the sphere is dependent on this equatorial velocity since the boundary layer separates around the equator. Therefore it determines the drag. From this point of view it seems to be reasonable to regard the mean velocity U_c in the smallest cross-section as the characteristic velocity. The length scale is the sphere diameter d_s. Since the tube diameter d_t appears as a second length scale, the similarity laws of

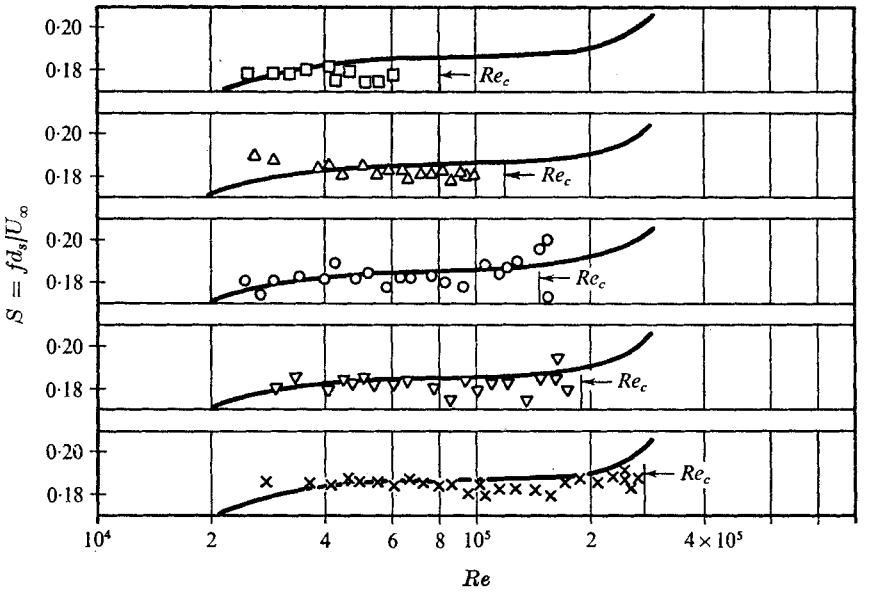

FIGURE 6. Strouhal number *vs.* Reynolds number for a sphere under various roughness conditions. ——, smooth (Achenbach 1974); symbols as in figure 2.

the flow yield an additional parameter, viz. the blockage ratio $B \equiv d_s/d_t$. In these terms the characteristics are defined as follows:

$$c_d = 4F/\tfrac{1}{2}\rho U_c^2 \pi d_s^2 \quad \text{(drag coefficient)},$$
$$Re = U_c d_s \rho/\eta \quad \text{(Reynolds number)},$$
$$B = d_s/d_t \quad \text{(blockage ratio)}.$$

ρ and η are the fluid density and fluid viscosity, respectively.

It is obvious that for $B \to 0$ the velocity U_c is equal to the velocity U_∞ of an infinite flow. Thus far the new definitions of the characteristics are compatible with those for an infinite flow.

In figure 7 the drag coefficient c_d is plotted as a function of the Reynolds number. The turbulence level was about $T = 0{\cdot}3\,\%$. The parameter varied is the blockage ratio $B \equiv d_s/d_t$. It is remarkable that even at the highest tunnel blockages the decrease in the drag coefficient at critical flow conditions is apparent. With increasing blockage ratio the subcritical drag coefficient as well as the critical Reynolds number increase. The lower limiting line represents the drag coefficient of a sphere in an 'infinite' flow. These results, which have been published previously by Achenbach (1972), were used as reference data. The drag coefficient measured for the highest blockage ratio under subcritical flow conditions is about twice the reference drag coefficient. In conventional terms and using the velocity of the oncoming flow as a reference value, this factor would be about 56. The triangles represent values obtained from integration of the local static pressure and skin-friction distribution around the circumference of the sphere at $d_s/d_t = 0{\cdot}916$. In this case the maximum velocities at the highest Reynolds number were of the order of half the velocity of sound and, thus, Mach number effects may be important.

The tests under the various blockage conditions have been carried out in an atmospheric air stream. For this reason the maximum Reynolds numbers are lower than those referring to infinite flows in the high-pressure wind tunnel.

At subcritical flow conditions the drag coefficient is nearly independent of the Reynolds number in the range tested. Thus the drag coefficient can be given as a function of the blockage ratio B. In figure 8 the experimental results are plotted in terms of $c_d/c_{d\infty}$ *vs.* B for $Re = 2 \times 10^5$. $c_{d\infty}$ denotes the corresponding drag coefficient for an infinite flow; its value is 0·51. The curve providing the best fit to the experimental results is

$$c_d/c_{d\infty} = 1 + 1{\cdot}45(d_s/d_t)^{4{\cdot}5}. \tag{1}$$

Equation (1) is experimentally confirmed for the blockage range $0{\cdot}5 < B < 0{\cdot}92$.

As mentioned above the character of the flow past spheres is unchanged even at the highest blockage ratios. This is illustrated in figure 9, where the local skin friction and static wall pressure are plotted as functions of the circumferential angle ϕ for the blockage ratio 0·916. The reference quantities are again the velocity U_c, the static pressure p_c, the density ρ and the viscosity η, all quantities referred to the smallest cross-section. In the immediate vicinity of the front stagnation point, the variation of the static pressure is small. The wall shear stress slowly increases with increasing distance from the front stagnation point. When $\phi > 50°$ the flow becomes more and more accelerated and causes an intensive pressure drop in the flow direction. At the same time the skin friction increases considerably and reaches a maximum value at $\phi = 80°$. The static pressure drops below the theoretical value calculated for the equatorial position ($\phi = 90°$) because of the effect of displacement by the tube boundary layer and the sphere boundary layer. The wall shear stress has already decreased for $\phi > 80°$, which means that the boundary layer on the sphere grows rapidly. At subcritical flow conditions the boundary layer separates laminarly at about $\phi = 100°$, such that the static pressure at the rear of the sphere is nearly equal to the theoretical value in the gap.

The curves representing the results for higher Reynolds numbers indicate by the resurgence of the skin friction the phenomena of laminar intermediate separation and turbulent reattachment of the boundary layer, as observed for the circular cylinder and sphere in an infinite flow. The downstream shift of the separation point causes a recovery of the static pressure at the rear of the sphere and hence a decrease in the drag coefficient.

The effect on the flow of an eccentric arrangement of the sphere in the tube is demonstrated in figure 10. The pressure and skin-friction distribution in a plane parallel to the main flow direction through the point of sphere–wall contact are plotted against the circumferential angle ϕ. The asymmetry of the distribution is obvious. The stagnation point is displaced about 15° towards the wall. For both Reynolds numbers the separation point near the wall is at about $\phi_s = 100°$, while in the opposite position the separation occurs at about $\phi_s = 125°$. It is remarkable that the boundary layer shows a supercritical behaviour at the large gap position (right side of figure 10) for a mass flow at which a subcritical Reynolds number is observed for the symmetric sphere arrangement. It is surprising that the pressure

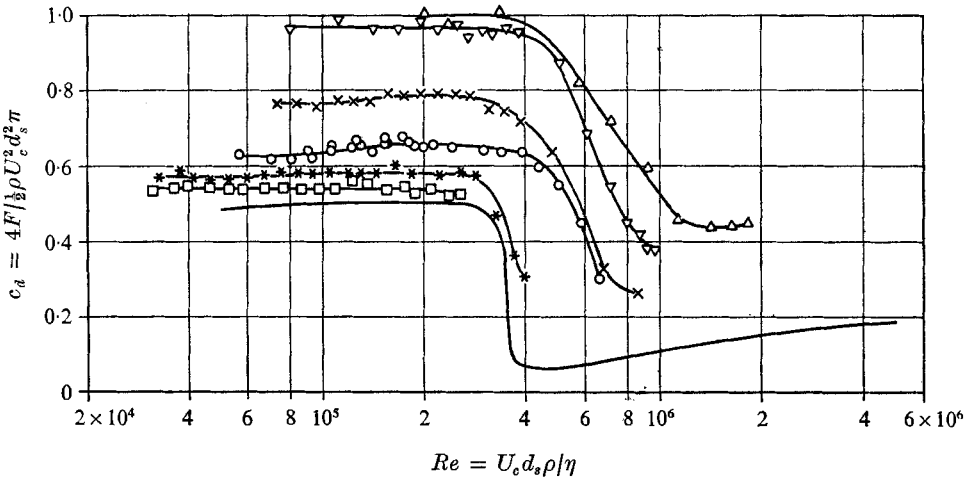

FIGURE 7. Drag coefficient *vs.* Reynolds number for a sphere at various blockage ratios. ——, $d_s/d_t = 0$ (Achenbach 1972); □, $d_s/d_t = 0{\cdot}5$; *, $d_s/d_t = 0{\cdot}6$; ○, $d_s/d_t = 0{\cdot}7$; ×, $d_s/d_t = 0{\cdot}8$; ▽, $d_s/d_t = 0{\cdot}9$; △, from integration, $d_s/d_t = 0{\cdot}916$.

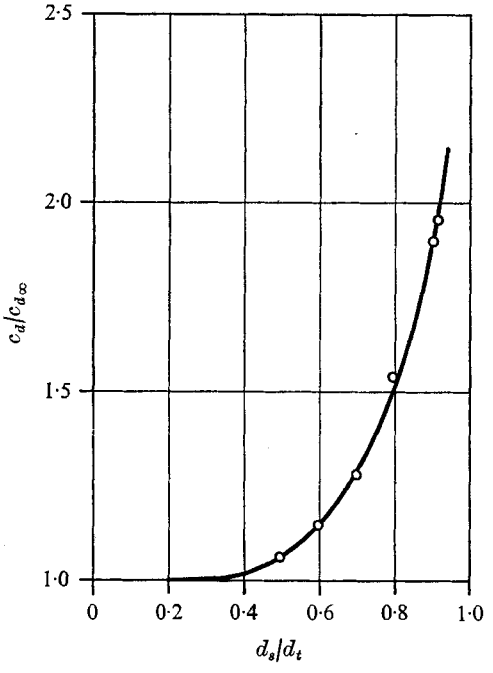

FIGURE 8. Effect of tunnel blockage on the drag for a sphere under subcritical flow conditions ($Re = 2 \times 10^5$). ——, $c_d/c_{d_\infty} = 1 + 1{\cdot}45(d_s/d_t)^{4{\cdot}5}$.

at the rear of the sphere and hence the drag coefficient are considerably different for both Reynolds numbers, though the skin-friction distributions are rather similar. This can be explained by the fact that the local quantities were measured only in one particular plane of the sphere. However, over the entire circumference the flow will be predominantly subcritical for the low and supercritical for the high Reynolds number.

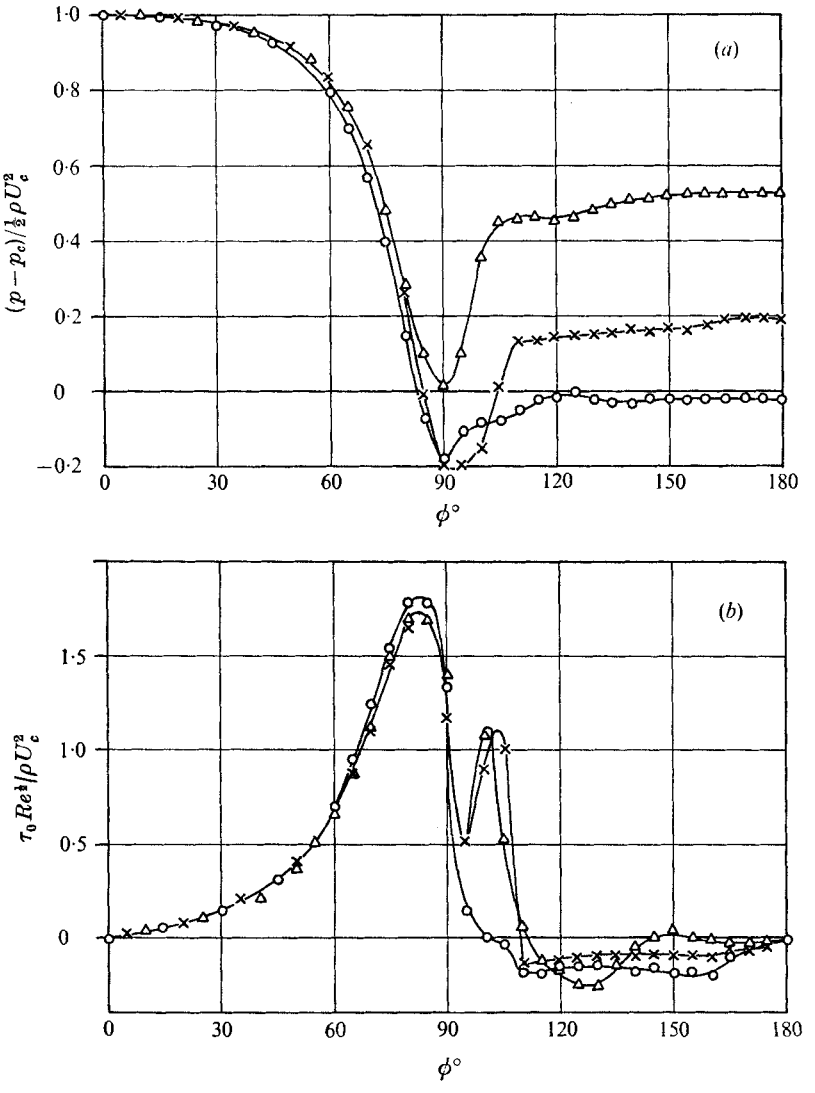

FIGURE 9. (*a*) Local static pressure and (*b*) skin-friction distribution for a sphere at the blockage ratio $d_s/d_t = 0{\cdot}916$. ○, $Re = 2\times10^6$; ×, $Re = 5{\cdot}7\times10^5$; △, $Re = 1{\cdot}4\times10^6$.

3.4. *Effect of turbulence level under conditions of high blockage*

The investigations of blockage effects have been carried out under the turbulence conditions of an entrance flow from quiescent air. A turbulence level of 0·3 % was determined from hot-wire measurements. Since a turbulence level of $T > 0{\cdot}3$ % was expected for the practical application to the pneumatic transport of spheres in a tube, T was increased in two steps without investigating the structure of the turbulence. In the first run a screen of wire diameter $d_w = 1$ mm and a 5 mm mesh size was employed. The turbulence level was determined to be 1·3 %. The second run was performed using a grid of flat wires 2·2 mm broad and a 7·5 mm mesh size. This arrangement yielded a turbulence level of 2·2 %. In

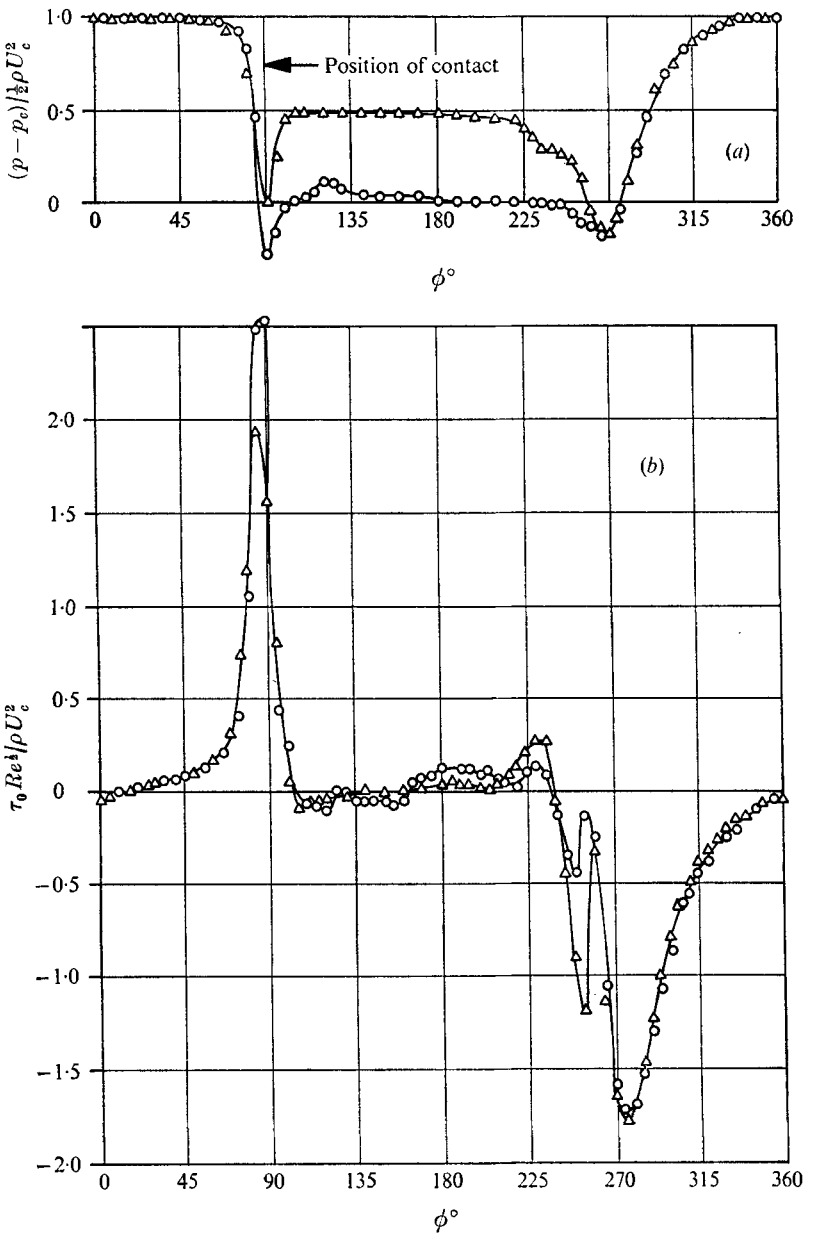

FIGURE 10. (*a*) Local static pressure and (*b*) skin-friction distribution for a smooth sphere arranged eccentrically at the blockage ratio $d_s/d_t = 0{\cdot}916$. ○, $Re = 2 \times 10^5$; △, $Re = 1{\cdot}4 \times 10^6$.

figure 11 the effect of different turbulence levels on the flow past spheres under the blockage condition $d_s/d_t = 0{\cdot}9$ is demonstrated. Increasing the turbulence level causes a premature transition from laminar to turbulent flow and hence a drop in the drag coefficient at lower Reynolds numbers.

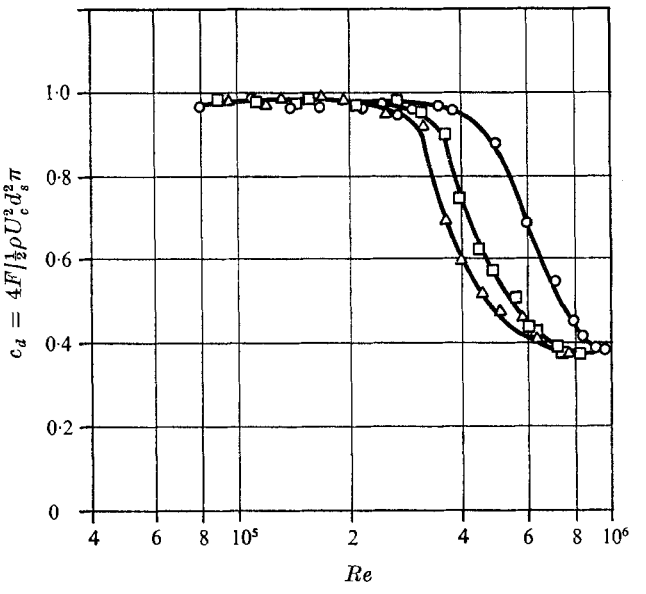

FIGURE 11. Effect of turbulence level T on the drag for a smooth sphere at the blockage ratio $d_s/d_t = 0{\cdot}9$. ○, $T = 0{\cdot}3$ %; □, $T = 1{\cdot}3$ %; △, $T = 2{\cdot}2$ %.

4. Final remarks

The surface of the sphere was roughened by being covered with small glass spheres as compactly as possible. In previous experiments on cross-flow past circular cylinders (Achenbach 1971) the same technique was employed. Comparison of these latter results with those obtained by Fage & Warsap (1930), who used emery paper to roughen the surface, indicated that the effective height k_{eff} of spherical roughness is not equal to the diameter k of the sphere but to $0{\cdot}55k$. This result is plausible as the lower hemisphere facing the test body is hardly wetted by the fluid flow. If this result is taken into account the present effective roughness parameters have the values $(k/d)_{\text{eff}} = 690 \times 10^{-5}, 275 \times 10^{-5}, 138 \times 10^{-5}$ and 83×10^{-5}. In figure 3 the second curve represents the dependency of the critical Reynolds number on the effective roughness parameter $(k/d)_{\text{eff}}$. As a further consequence of the experimental technique, the effective diameter of the test body is equal to the true diameter plus $0{\cdot}9k$. This effective diameter has been employed in the present evaluation of the results.

The determination of the mass flow for the experiments on the blockage effect has been a problem. The intention to put the sphere into the entrance region of the flow so that it might experience a plane velocity profile conflicted with the need to measure the static pressure of the undisturbed flow upstream of the sphere at a position as far from the sphere as possible. In addition very small pressure differences occurred, particularly for the tests at high blockage conditions. In preliminary tests the arrangement problems were optimized experimentally by minimizing the distances according to figure 1. The small pressure differences were measured by means of a high-precision bourdon-tube pressure gauge (Texas Instruments, Houston).

Finally, an unexpected effect should be mentioned. At critical flow conditions the sphere was pushed by lift forces towards the wall of the tube. This movement grew more and more intense as the critical Reynolds number was approached. Occasionally the sphere rolled on its equator along the inner circumference of the tube like the inner wheel of an epicyclic gear. The tension in the mounting wire became very small. It appeared that the drag force more or less vanished. This flow state could not be terminated by increasing the mass flow. The phenomenon described could not be studied in detail. However, an attempt will be made to explain its initiation. In the critical flow range a small variation in the Reynolds number causes a drastic change in the drag coefficient. This change is due to a downstream shift of the boundary-layer separation point accompanied by a recovery of the static pressure at the rear of the sphere. The flow state is rather unstable and therefore any slight asymmetry of the geometry due to eccentricity or individual surface roughness would cause a local premature transition of the boundary layer. The resulting three-dimensional pressure distribution yields a force perpendicular to the main flow direction which drives the sphere towards the wall. Since the sphere is in contact with the wall of the tube, it tends to stay there. A pressure distribution as illustrated in figure 10 builds up and supplies a transverse force which holds the sphere against the wall. The force parallel to the main flow direction is compensated for at the wall by static friction forces between the sphere and the tube. Thus the drag appears to have vanished. Usually the transverse force does not act in a plane containing the point of contact and the centre of the sphere. In this case the sphere would experience a moment of torque which would cause it to roll. That this motion, once started by a random event, continues is not easy to see. Possibly effects quite different from those investigated here become relevant. In any case, the asymmetric boundary-layer separation will be sustained. It would move in the sense opposite to the rotation of the sphere like the transverse force, which supports the rotation and whose direction and magnitude remain steady relative to the point of contact.

The present results were carried out in the laboratories of the Institut für Reaktorbauelemente, Kernforschungsanlage Jülich GmbH. The director of the Institute, Dr C. B. von der Decken, supported this work with great interest. The author wishes to thank him very much. He also wishes to express his gratitude to his assistants H. Gillessen, F. Hoffmanns, H. Reger, R. Rommerskirchen and W. Schmidt for their valuable help during the preparation and execution of the tests.

REFERENCES

ACHENBACH, E. 1971 Influence of surface roughness on the cross-flow around a circular cylinder. *J. Fluid Mech.* **46**, 321–335.

ACHENBACH, E. 1972 Experiments on the flow past spheres at very high Reynolds numbers. *J. Fluid Mech.* **54**, 565–575.

ACHENBACH, E. 1974 Vortex shedding from spheres. *J. Fluid Mech.* **62**, 209–221.

FAGE, A. & WARSAP, J. H. 1930 The effect of turbulence and surface roughness on the drag of a circular cylinder. *Aero. Res. Counc. R. & M.* no. 1283.